Assignment of Backbone Resonances for Larger Proteins Using the $^{13}C-^{1}H$ Coherence of a $^{1}H_{\alpha}$-, ^{2}H-, ^{13}C-, and ^{15}N-Labeled Sample

Toshio Yamazaki,* Hidehito Tochio, Junichi Furui, Saburo Aimoto, and Yoshimasa Kyogoku

Contribution from the Institute for Protein Research, Osaka University, 3-2 Yamadaoka, Suita, Osaka 565, Japan

Received August 21, 1996[⊗]

Abstract: A suite of triple resonance NMR experiments for the assignment of backbone resonances of a larger protein using selectively $^{1}H_{\alpha}$ labeling to a sample uniformly labeled with ^{13}C, ^{15}N, and ^{2}H is described. The relaxation time of $^{1}H_{\alpha}-^{13}C_{\alpha}$ zero/double quantum coherence was more than 4 times as long as that of $^{13}C_{\alpha}$ single quantum coherence. Three-dimensional HACAN, HACACB, HACACO, and HACA(N)CO experiments were newly designed to utilize selectively labeled $^{1}H_{\alpha}$ nuclei. HACAN provides intraresidue and sequential connectivities through amide ^{15}N spins. HACACO and HACA(N)CO provide intraresidue and sequential connectivities through ^{13}CO spins. HACACB provides connectivity to $^{13}C_{\beta}$, giving the type of amino acid. Long-life $^{1}H_{\alpha}-^{13}C_{\alpha}$ zero/double quantum coherence provides high sensitivity in these NMR experiments. Except for a few amino acid type-specific problems, all sequential connectivities were obtained for a test sample of a 98 amino acid protein at 10 °C, which rotationally diffuses with a correlation time of 17 ns, corresponding to an over 30 kDa protein at 30−40 °C. Zero/double quantum based triple resonance experiments and $^{1}H_{\alpha}$ selective labeling provide a new approach for NMR studies on larger proteins.

Introduction

Recent progress in triple resonance NMR techniques has allowed the assignment of individual resonances and the determination of the solution structures of proteins of up to ∼25 kDa. One of the problems with proteins larger than this is that the faster relaxation of transverse magnetization impairs the resolution of resonance peaks and the efficiency of magnetization transfer in complicated triple resonance experiments. As a solution of this problem, fractional and nonselective ^{2}H labeling as well as uniform ^{13}C and ^{15}N labeling was proposed, first for backbone resonance assignment.[1−7] The assignment of side chain resonances[8−10] and the measurement of structural information[10−12] were also partly achieved using ^{2}H-labeled samples. Measurement of the relaxation of deuteron magnetization has also shown great capability as to the elucidation of side chain dynamics.[13]

A large part of the relaxation of ^{13}C magnetization is attributed to the dipole−dipole interaction between ^{1}H and ^{13}C spins. By replacing ^{1}H, which has a large magnetic moment, by ^{2}H, which has a smaller one, a great reduction in the transverse relaxation rate of ^{13}C magnetization has been obtained. As demonstrated for a 37 kDa protein/DNA complex, the average T_2 of $^{13}C_{\alpha}$ magnetization was 16 ms for a protonated sample and 130 ms for a deuterated one.[3] The increased life time of magnetization was fully utilized in modified triple resonance experiments, CT-HNCA, CT-HN(CO)CA, HN(CA)-CB, and HN(COCA)CB. This set of triple resonance experiments allowed us to assign the backbone resonances ($^{1}H_{N}$, ^{15}N, $^{13}C_{\alpha}$, and $^{13}C_{\beta}$) of a 37 kDa Trp repressor/operator DNA complex. Recently, the assignment of backbone resonances of a 64 kDa complex was also achieved with this set of experiments and an extension of them.[7]

A drawback of ^{2}H labeling is the loss of ^{1}H nuclei, which provide structural information through NOE experiments. Though nonselective deuteration gave excellent results for the backbone resonance assignment, a strategy for the resonance assignment of ^{13}C-attached ^{1}H spins and structure determination has not yet been established. As the first step, this paper shows that a $^{1}H-^{13}C$ pair can exhibit long-life coherence if all ^{1}H spins around a selected ^{1}H are replaced by ^{2}H. New methods involving a $^{1}H_{\alpha}$-labeled protein are demonstrated here because of the ease of labeling at H_{α} and their usefulness for backbone assignment. Selective ^{1}H labeling is a possible approach for obtaining ^{1}H resonance assignments and structural information on the basis of the ^{1}H resonances for larger proteins.

* To whom correspondence should be addressed. Telephone: +81-6-879-8598. Fax: +81-6-879-8599. E-mail: yamazaki@protein.osaka-u.ac.jp.

[⊗] Abstract published in *Advance ACS Abstracts,* January 1, 1997.

(1) Grzesiek, S.; Anglister, J.; Ren, H.; Bax, A. *J. Am. Chem. Soc.* **1993**, *115*, 4369−4370.

(2) Yamazaki, T.; Lee, W.; Revington, M.; Mattiello, D. L.; Dahlquist, F. W.; Arrowsmith, C. H.; Kay, L. E. *J. Am. Chem. Soc.* **1994**, *116*, 6464−6465.

(3) Yamazaki, T.; Lee, W.; Arrowsmith, C. H.; Muhandiram, D. R.; Kay, L. E. *J. Am. Chem. Soc.* **1994**, *116*, 11655−11666.

(4) Venters, R. A.; Huang, C.; Farmer II, B. T.; Trolard, R.; Spicer, L. D.; Fierke, C. A. *J. Biomol. NMR* **1995**, *5*, 339−344.

(5) Matsuo, H.; Li, H.; Wagner, G. *J. Magn. Reson.* **1996**, *B 110*, 112−115.

(6) Shirakawa, M.; Waelchli, M.; Shimizu, M.; Kyogoku, Y. *J. Biomol. NMR* **1995**, *5*, 323−326.

(7) Shan, X.; Gardner, K. H.; Muhandiram, D. R.; Rao, N. S.; Arrowsmith, C. H.; Kay, L. E. *J. Am. Chem. Soc.* **1996**, *118*, 6570−6579.

(8) Farmer II, B. T.; Venters, R. A. *J. Am. Chem. Soc.* **1995**, *117*, 4187−4188.

(9) Farmer II, B. T.; Venters, R. A. *J. Biomol. NMR* **1996**, *7*, 59−71.

(10) Nietlispach, D.; Clowes, R. T.; Broadhurst, R. W.; Ito, Y.; Keeler, J.; Kelly, M.; Ashurst, J.; Oschkinat, H.; Domaille, P. J.; Laue, E. D. *J. Am. Chem. Soc.* **1996**, *118*, 407−415.

(11) Grzesiek, S.; Wingfield, P.; Stahl, S.; Kaufman, J. D.; Bax, A. *J. Am. Chem. Soc.* **1995**, *117*, 9594−9595.

(12) Venters, R. A.; Metzler, W. J.; Spicer, L. D.; Mueller, L.; Farmer, B. T. *J. Am. Chem. Soc.* **1995**, *117*, 9592−9593.

(13) Muhandiram, D. R.; Yamazaki, T.; Sykes, B.; Kay, L. E. *J. Am. Chem. Soc.* **1995**, *117*, 11536−11544.

S0002-7863(96)02945-9 CCC: $14.00

Transverse magnetization of ^{13}C attached by ^{1}H decays very quickly, as mentioned above, but the double and zero quantum coherences of a $^{13}C-^{1}H$ pair can survive longer. The $^{13}C-^{1}H$ dipolar interaction causes little relaxation of the double/zero quantum coherence in the case of a large molecule, because the secular part of the dipolar Hamiltonian does not cause splitting of these coherences of the heteronuclear half-spin pair.[14] The advantage of the double/zero quantum coherence was originally demonstrated for $^{15}N-^{1}H$ spin pairs.[15] Greater benefit was expected for $^{13}C-^{1}H$ spin pairs. These long-life coherences can be used in many types of triple resonance experiments simply by replacing the heteronuclear single quantum correlation (HSQC) scheme by the heteronuclear multiple quantum correlation (HMQC) scheme.[16] However, a problem with this idea is that the transverse ^{1}H component of the double/zero quantum coherence is coupled with other surrounding ^{1}H nuclei through dipole−dipole and scalar coupling mechanisms, as the pure ^{1}H transverse magnetization is. The scalar coupling interaction causes a cosine-shaped signal decay, and the dipole−dipole interaction causes an exponential decay. The scalar coupling interaction can be largely suppressed by ^{1}H spin-locking, by which the $^{1}H_{\alpha}$ component of the double/zero quantum coherence is spin-locked and decoupled from $^{1}H_{\beta}$ nuclei. Using this scheme, several useful applications have been demonstrated.[17,18] The suppression of the homonuclear scalar coupling interaction depends strongly on the offsets of resonance frequencies of the coupled spins from the irradiation frequency. When absolute values of offsets of the coupled spins are similar to each other, so called the Hartmann−Hahn matching condition, the signal will be lost through magnetization transfer to neighboring spins. Decoupling by spin-locking has also been used in $^{13}C_{\alpha}$ relaxation measurement experiments,[19] which gave successful results except for some Ser residues. In the case of ^{1}H nuclei, the distributions of H_{α} and H_{β} chemical shifts overlap each other. Undesired magnetization transfer can occur for some H_{α} and H_{β} pairs. On the other hand, the transverse relaxation caused by the $^{1}H-^{1}H$ dipolar interaction cannot be suppressed by any pulse techniques. The only perfect way to achieve long-life double/zero quantum coherence is the deuteration of all ^{1}H nuclei other than $^{1}H_{\alpha}$. A $^{1}H_{\alpha}-^{13}C_{\alpha}$ correlation experiment with high resolution in both the ^{13}C and ^{1}H dimensions with a ^{13}C,^{1}H-dual constant time scheme was also achieved using this sample, which will be reported separately.

The long-life coherence of $^{13}C_{\alpha}$ can be used for the correlation of neighboring spins through scalar coupling such as $^{13}C_{\alpha}-^{15}N$ and $^{13}C_{\alpha}-^{13}CO$. By combining correlation experiments for different backbone nuclei, the sequential assignments of backbone resonances are made. Experiments for obtaining sequential connectivities starting from $^{13}C_{\alpha}$, 2D HA(CA)N and HA(CACO)N, have already been proposed.[20] HA(CA)N gives connectivity from $^{1}H_{\alpha}$ to amide ^{15}N in the same residue and to that in the next residue. HA(CACO)N gives connectivity to the amide ^{15}N in the next residue exclusively. These pulse sequences include $^{13}C_{\alpha}$ single quantum coherence periods of about 50 ms. Since the relaxation time of the $^{13}C_{\alpha}$ single quantum coherence is as short as 13 ms for the current sample, the magnetization decays completely during these periods. By replacing the HSQC scheme in these pulse sequences by the HMQC scheme utilizing the long-life $^{13}C-^{1}H$ double/zero quantum coherence obtained by $^{1}H_{\alpha}$ selective labeling, a highly sensitive version of HACAN was designed. On the other hand, HA(CACO)N still fails even with modification with the HMQC scheme, because the fast relaxation of the ^{13}CO spin produced by chemical shift anisotropy cannot be reduced by deuteration of protein samples or any pulse techniques. Instead, a 3D HACA(N)CO experiment is proposed here, which connects $^{13}C_{\alpha}$ through ^{15}N to ^{13}CO in the previous residue. Because the ^{15}N spin relaxes slower than the ^{13}CO spin, especially when ^{2}H is attached to it and decoupled by ^{2}H irradiation, the correlation from ^{15}N to ^{13}CO used in HACA(N)CO is much more sensitive than that from ^{13}CO to ^{15}N used in HA(CACO)N. Intraresidue $^{1}H-^{13}C_{\alpha}-^{13}CO$ connectivities are given by HACACO, which is also modified with the $^{13}C-^{1}H$ double/zero quantum coherence for sensitivity improvement for large proteins. Through these two experiments, $^{1}H-^{13}C$ pairs in the neighboring residues are connected through ^{13}CO. Additionally, an HMQC version of HACACB is proposed here, which gives intraresidue $^{1}H_{\alpha}-^{13}C_{\alpha}-^{13}C_{\beta}$ connectivities for identification of the amino acid type. A combination of the four experiments yields enough information for backbone resonance assignments.

The sample we used is the C-terminal domain of the α subunit of *Escherichia coli* RNA polymerase consisting of 98 amino acid residues.[21] To test the effectiveness of the newly developed isotope labeling and NMR methods for larger proteins, all the experiments were performed at a low temperature, 10 °C. As judged from the T_2 values of $^{13}C_{\alpha}$ nuclei, the overall tumbling rate of this molecule at 10 °C was similar to that of an over 30 kDa protein at 30−40 °C. We demonstrate the newly developed methods using this molecule.

Methods

An amino acid mixture triply labeled with ^{15}N, ^{13}C, and ^{2}H was purchased from Cambridge Isotope Laboratory Inc. For $^{1}H_{\alpha}$ labeling, we followed the procedure developed for ^{3}H labeling for determination of the C-terminal amino acid of a polypeptide[22,23] using $^{1}H_2O$ in place of $^{3}H_2O$. To a solution of 0.25 g of the labeled amino acid mixture in 6 mL of $^{1}H_2O$ and 12 mL of pyridine in an ice bath was added 12 mL of acetic anhydride, followed by incubation in a water bath at 20 °C for 15 min. After cooling again in the ice bath, 24 mL of pyridine and 24 mL of acetic anhydride were added, and the mixture was incubated in the water bath at 20 °C for 1 h. Then 6 mL of H_2O was added, and the incubation was continued for a further 1 h. The solvent was removed using a rotary evaporator. The acetylated amino acid mixture was dissolved in 6 N hydrogen chloride, degassed, and then sealed in glass tubes. The deacetylation reaction was performed at 100 °C for 10 h. The solvent was removed by evaporation. The $^{1}H_{\alpha}$ labeled amino acid mixture was dissolved in H_2O, its pH was adjusted to 7, and then it was mixed into the culture medium.

The C-terminal domain of the α subunit of *E. coli* RNA polymerase was overexpressed using a pGEM/BL21(DE3) system and purified as described previously.[21] This fragment consists of 98 amino acids starting from Asp233, with Met at the N-terminus. A sample labeled with ^{13}C and ^{15}N was produced using M9 culture medium with 1.5 g/L [^{13}C]glucose and 0.5 g/L [^{15}N]ammonium chloride. A sample labeled selectively at H_{α} with ^{1}H as well as uniformly with ^{13}C, ^{15}N, and ^{2}H was produced as follows. *E. coli* was amplified to an absorbance of close to 0.8 at 600 nm in 200 mL of M9 culture medium containing

(14) Griffey, R. H.; Redfield, A. G. *Q. Rev. Biophys.* **1987**, *19*, 51−82.
(15) Bax, A.; Kay, L. E.; Sparks, S. W.; Torchia, D. A. *J. Am. Chem. Soc.* **1989**, *111*, 408−409.
(16) Seip, S.; Balbach, J.; Kessler, H. *J. Magn. Reson.* **1992**, *100*, 406−410.
(17) Grzesiek, S.; Kuboniwa, H.; Hinck, A. P.; Bax, A. *J. Am. Chem. Soc.* **1995**, *117*, 5312−5315.
(18) Grzesiek, S.; Bax, A. *J. Biomol. NMR* **1995**, *6*, 335−339.
(19) Yamazaki, T.; Muhandiram, R.; Kay, L. E. *J. Am. Chem. Soc.* **1994**, *116*, 8266−8278.
(20) Wang, A.; Grzesiek, S.; Tschudin, R.; Lodi, J.; Bax, A. *J. Biomol. NMR* **1995**, *5*, 376−382.
(21) Jeon, Y. H.; Negishi, T.; Shirakawa, M.; Yamazaki, T.; Fujita, N.; Ishihama, A.; Kyogoku, Y. *Science* **1995**, *270*, 1495−1497.
(22) Matsuo, H.; Narita, K. *Protein Sequence Determination*; Springer-Verlag: Berlin, 1975; pp 104−113.
(23) Narita, K.; Matsuo, H.; Nakajima, T. *Protein Sequence Determination*; Springer-Verlag: Berlin, 1975; pp 30−103.

1.5 g/L [^{13}C]glucose and 0.5 g/L [^{15}N]ammonium chloride. The cells were collected by centrifugation, and then resuspended in 50 mL of M9 culture medium containing 0.5 g/L [^{13}C]glucose, 0.5 g/L [^{15}N]-ammonium chloride, and 5 g/L $^{1}H_{\alpha}$-labeled [^{13}C]-, [^{15}N]-, and [^{2}H]-amino acid mixture. After 30 min of incubation, induction was initiated by adding IPTG and continued for 3 h. For each sample, the protein was dissolved to a concentration of 1.5 mM in $^{2}H_2O$ with 20 mM potassium phosphate and 30 mM KCl adjusted to pH 6.0.

All relaxation experiments were performed with a 600 MHz JEOL Alpha spectrometer. The relaxation rates of the transverse magnetization of $^{13}C_{\alpha}$ nuclei were measured in a series of 2D $^{13}C-^{1}H$ correlation experiments using the pulse sequence explained under Results and Discussion. Each 2D experiment was performed with $^{13}C_{\alpha}$ transverse magnetization relaxation periods of 6, 12, 18, and 30 ms. The common parameters were as follows. The spectral center and width were 4.45 ppm and 10 000 Hz for the ^{1}H axis and 58.2 ppm and 5000 Hz for the ^{13}C axis. For the ^{1}H and ^{13}C axes, respectively, 512 × 128 hypercomplex points were collected, giving resolutions of 9.8 and 19.5 Hz after zero filling. For each 1D FID, 32 transients were accumulated with a 1.5 s repetition interval, the total experiment time for four 2D experiments being 14 h.

The relaxation rates of the zero/double quantum coherences of $^{13}C_{\alpha}-^{1}H_{\alpha}$ pairs were measured under the same conditions except for the following parameters. The lengths of the zero/double quantum relaxation period were 10, 20, 30, and 50 ms. Three sets of experiments with different ^{13}C carrier positions, i.e., 51.2, 58.2, and 65.2 ppm, were performed to eliminate the offset problem explained under Results and Discussion. Peak intensities were taken from the spectrum giving the smallest offset. For each 1D FID, 16 transients were accumulated with a 1.5 s repetition interval, giving a total time of 21 h for 12 2D experiments.

All backbone correlation experiments were performed with a 500 MHz Bruker DMX500 spectrometer. For the HACAN experiment, the spectral center and width were 4.28 ppm and 8012.8 Hz for f_3 ($^{1}H_{\alpha}$), 57.5 ppm and 2000 Hz for f_1 ($^{13}C_{\alpha}$), and 118.3 ppm and 1000 Hz for f_2 (^{15}N). A total of 32 (t_1) × 64 (t_2) × 512 (t_3) 3D complex points were collected. For each 1D FID, eight transients were accumulated with a 2 s repetition interval. The total experiment time was 40 h. The t_1 dimension was extrapolated to 64 points by mirror image linear prediction. Data were zero-filled and Fourier transformed, giving resolutions of 15.6 Hz (f_1), 7.8 Hz (f_2), and 7.8 Hz (f_3). The same data processing was applied to all the following 3D experiments.

For the HACACO experiment, the spectral center and width were 4.28 ppm and 8012.8 Hz for f_3 ($^{1}H_{\alpha}$), 57.5 ppm and 2000 Hz for f_1 ($^{13}C_{\alpha}$), and 176.5 ppm and 1200 Hz for f_2 (^{13}CO). A total of 50 (t_1) × 32 (t_2) × 512 (t_3) 3D complex points were collected. For each 1D FID, eight transients were accumulated with a 1 s repetition interval. The total experiment time was 10 h. The resolution of f_2 was 18.8 Hz.

For the HACACB experiment, the spectral center and width were 4.28 ppm and 8012.8 Hz for f_3 ($^{1}H_{\alpha}$), 58.4 ppm and 2000 Hz for f_1 ($^{13}C_{\alpha}$), and 42.5 ppm and 8000 Hz for f_2 ($^{13}C_{\beta}$). A total of 32 (t_1) × 64 (t_2) × 512 (t_3) 3D complex data points were collected. For each 1D FID, eight transients were accumulated with a 1 s repetition interval. The total experiment time was 20 h. The resolution of f_2 was 62.5 Hz.

For the HACA(N)CO experiment, the spectral center and width were 4.28 ppm and 8012.8 Hz for f_3 ($^{1}H_{\alpha}$), 57.5 ppm and 2000 Hz for f_1 ($^{13}C_{\alpha}$), and 176.5 ppm and 1200 Hz for f_2 (^{13}CO). A total of 32 (t_1) × 32 (t_2) × 512 (t_3) 3D complex points were collected. A total of 16 transients were accumulated for each 1D FID with a 2 s repetition interval. The total experiment time was 40 h. The resolution of f_2 was 18.8 Hz.

Because of the dilution of protons for the deuterated sample, the longitudinal relaxation time becomes longer. For all the above experiments, a 2 s repetition interval would give the highest sensitivity per experimental time, which was determined in HMQC experiments with different repetition intervals. A larger number of increments for the $^{13}C_{\alpha}$ axis, up to 84 points for HACACB and up to 50 points for others, is acceptable for higher resolution, though it was shortened for reduction of the experimental times in this study.

Results and Discussion

Preparation of a Selectively-$^{1}H_{\alpha}$-Labeled Protein. A protein sample labeled selectively at H_{α} with ^{1}H as well as uniformly with ^{13}C, ^{15}N, and ^{2}H was produced by using the *E. coli* overproduction system in M9 minimal culture medium containing amino acids selectively $^{1}H_{\alpha}$ labeled and uniformly labeled with ^{13}C, ^{15}N, and ^{2}H. The amino acids were obtained by replacing $^{2}H_{\alpha}$ with ^{1}H in the uniformly-^{13}C-, -^{15}N-, and -^{2}H-labeled amino acid mixture. Several methods are available for the replacement of H_{α}.[24] We chose racemization accompanied by acetylation. A mixture of acetylated amino acids was converted to amino acids by hydrolysis. The yield of each type of amino acid was estimated from the $^{1}H-^{1}H$ COSY and $^{1}H-^{13}C$ HSQC spectra of the amino acid mixture in which $^{1}H_{\alpha}$ was replaced by ^{2}H, starting from an unlabeled amino acid mixture. Cys, Trp, Gln, and Asn had already been lost, because the commercially obtained amino acid mixture was produced by hydrolysis of protein. The racemization reaction cannot be applied to Pro, Ser, and Thr. The hydroxyl groups of Ser and Thr were degraded. For Pro, nothing happened because the oxazolone ring as a racemization intermediate cannot be formed. More than 70% of H_{α} of Glu and Asp remained unchanged. For 11 other amino acids, $^{1}H_{\alpha}$ selective labeling was achieved. At least 80% of the H_{α} of these amino acids was replaced. Another method of acetylation using acetic anhydride and water at a higher temperature (170 °C)[25] was also tested. As reported, Pro was also acetylated and H_{α} of Pro was also replaced. The reported reaction time of 2 min, however, was not sufficient for the complete replacement of $^{1}H_{\alpha}$. Ser and Thr were again lost. Several unknown degradation products were generated from other amino acids, but they were not fully analyzed. This method might be better than the former one if the conditions for the reaction of the amino acid mixture are optimized, but we did not attempt this in the current study.

The intake of amino acids from the culture medium by *E. coli* is another hurdle in the labeling of proteins. To determine the minimal concentration of the labeled amino acid mixture in the culture medium required for sufficient intake, we measured the reduction of the peak intensities in a $^{13}C-^{1}H$ 2D correlation spectrum of a protein sample made in the culture medium with various amounts of a deuterated amino acid mixture. We found that 3 g of the amino acid mixture per liter of culture was required for more than 80% labeling of most amino acids, though Glu, Asp, and Ser were labeled less than 20%, and half of Ala and three-quarters of Thr were labeled by ^{2}H amino acids in the culture. Note that we did not observe position-specific protonation (e.g., H_{α}), which could be caused by metabolism of amino acids. All the peaks for the same amino acid decreased in their intensity similarly. For the preparation of a [^{15}N]-, [^{13}C]-, [^{2}H]-, and [$^{1}H_{\alpha}$]protein, double the amount of the labeled amino acids, which was racemized, would be required in the culture medium for the same level of labeling, since D-amino acids (stereoisomers) would not be incorporated. Though a few D-amino acids could be used after interconversion by racemases, we did not perform experiments to estimate this effect. In an actual sample preparation, 5 g of amino acid mixture per liter of culture was used. To reduce the consumption of expensive labeled amino acids, *E. coli* was amplified in 200 mL of ^{13}C- and ^{15}N-labeled M9 medium without amino acids, collected by centrifugation, and then resuspended in 50 mL of the culture medium containing the labeled amino acids. This gave 4 mg of protein. Whether each residue is protonated or deuterated

(24) LeMaster, D. M. *Prog. NMR Spectrosc.* **1994**, *26*, 371−419.
(25) Upson, D. A.; Hruby, V. J. *J. Org. Chem.* **1977**, *42*, 2329−2330.

at H_β can be judged from the two-bond isotope shift of $^{13}C_\alpha$ (roughly -0.1 ppm/substitution of H_β) and the three-bond isotope shift of $^1H_\alpha$ (roughly -0.01 ppm/substitution of H_β) observed in $^{13}C-^1H$ correlation spectra recorded with long ^{13}C acquisition times. These isotope shifts were not evident in the 3D spectra described below. Probably because of the higher concentration of *E. coli*, the supply of Arg did not seem sufficient. Only half of the Arg was taken from the culture medium and labeled. The rest of the Arg was protonated at H_β, probably fully. For Phe, His, Ile, Lys, Leu, Met, Val, and Tyr, peaks of those protonated at H_β were not observed, which means they were labeled at least 80%, as expected. Ala and Thr were labeled similarly to those in the test run. Pro was completely deuterated. For Gly residues, both H_α nuclei were protonated. The double/zero quantum coherence of $^{13}C_\alpha$ and one of the two $^1H_\alpha$ spins of Gly relax quickly due to the dipolar interaction with the other $^1H_\alpha$ spin. The stereospecific deuteration of H_α nuclei of Gly[26,27] must be useful, but it was not applied in this study.

Relaxation Measurements. The transverse relaxation times of the $^{13}C_\alpha$ single quantum coherence and $^{13}C_\alpha-^1H_\alpha$ double/zero quantum coherence were measured using newly developed pulse sequences, as shown in Figure 1, giving 2D $^{13}C-^1H$ correlation spectra. For the measurement of the $^{13}C_\alpha$ single quantum coherence relaxation time, the previously designed pulse sequence[19] was modified by employing the double/zero quantum coherence instead of the ^{13}C single quantum coherence during the constant time ^{13}C chemical shift evolution period, giving higher sensitivity. The relaxation rates for the double/zero quantum coherences of $^{13}C_\alpha-^1H_\alpha$ were measured by applying continuous waves for locking both spins and removing $^1H-^1H$ and $^{13}C-^{13}C$ homonuclear scalar couplings. As pointed out, partial scalar coupling of the $^1H-^{13}C$ spin pair caused by an off-resonance effect can evolve, while ^1H only spin-locking is applied to the double/zero quantum coherence. However, in the case of double spin-locking on ^{13}C and ^1H nuclei, the double/zero quantum coherence is locked along the effective rotation axes. If the amplitudes of both ^{13}C and ^1H spin-locking are far greater than the $^1H-^{13}C$ scalar coupling, the locked product term, of which the ^{13}C and ^1H components are along the ^{13}C and ^1H effective fields, is not perturbed by the scalar coupling. This is true even when the rates of the two effective rotations are similar. The Hamiltonian is written as

$$H = \omega_H H_Z + \omega_{rfH} H_X + \omega_C C_Z + \omega_{rfC} C_X + J H_Z C_Z$$

where J is the coupling constant between the H and C spins, ω_H and ω_C are their offsets from the applied RF for ^1H and ^{13}C, and ω_{rfH} and ω_{rfC} are the amplitudes of the applied RF. In the doubly tilted frame, the Hamiltonian is approximated as

$$H \approx \omega_{effH} H_{Z'} + \omega_{effC} C_{Z''} + J(\sin\theta_C)(\sin\theta_H) H_{Z'} C_{Z''} + J(\cos\theta_H)(\cos\theta_C)(H_{X'} C_{X''} + H_{Y'} C_{Y''})/2$$

where Z' and Z'' represent the directions of the effective rotation axes for ^1H and ^{13}C, respectively, ω_{effH} and ω_{effC} are the effective rotation rates for ^1H and ^{13}C, respectively, and θ_H and θ_C represent the tilt angles from the X axis as to the Z' and Z'' axes, respectively. All other scalar coupling terms are nonsecular and neglected under the condition that ω_{effC}, $\omega_{effH} \gg |J|$. The last term can also be neglected when the effective rotation rates of ^1H and ^{13}C differ greatly. The $H_{Z'}C_{Z''}$ term is not perturbed by the effective Hamiltonian in either case.

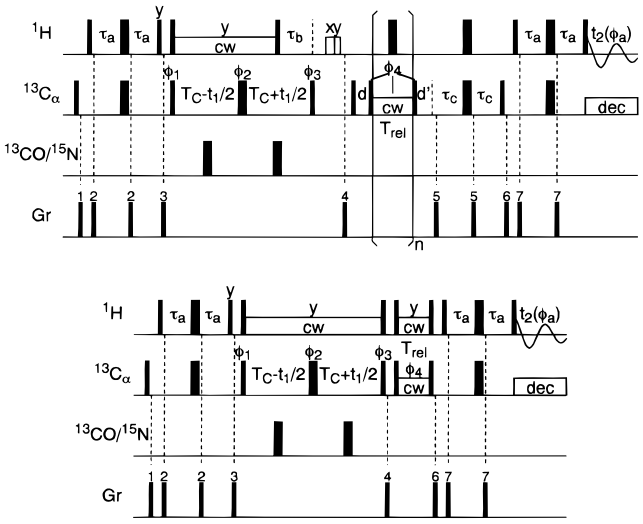

Figure 1. (a, top) Pulse sequence for measuring $^{13}C_\alpha$ single quantum relaxation rates. The ^1H channel is positioned at 4.45 ppm and the ^{13}C channel at 58.2 ppm. The thin and thick bars represent the $\pi/2$ and π pulses, respectively. All pulses without phase are applied along the x-axis. The delays are set as follows: $\tau_a = 1.7$ ms, $T_C = 14.3$ ms, $\tau_b = 3.4$ ms, $\tau_c = 1.5$ ms, $T_{rel} = 6$ ms, $d = 1/\omega_{CSL} - (4/\pi)\tau_{C90}$, $d' = 1/\omega_{CSL}$, where ω_{CSL} is the amplitude of ^{13}C spin-locking in the T_{rel} period and τ_{C90} is the ^{13}C $\pi/2$ pulse width. The ^1H $\pi/2$ pulse width is 6.5 μs and the ^{13}C $\pi/2$ pulse width is 18.5 μs at the full power of each channel. The amplitude of ^1H spin-locking by a continuous wave during the T_C period is 5.2 kHz. The amplitude of ^{13}C spin-locking by a continuous wave during the T_{rel} period is 3.1 kHz. The MPF5 ^{13}C decoupling sequence[29,30] during the ^1H acquisition period is applied at an amplitude of 2.1 kHz. The ^{13}CO pulses are generated from the ^{13}C channel by phase modulation and are centered at 179.2 ppm. The selective π pulse with a Gaussian shape is applied, of which the peak amplitude is 4.7 kHz. The ^{15}N channel is positioned at 120 ppm, and the π pulses of 68 μs at the full power are applied. Both the ^{13}CO and ^{15}N π pulses are located at the midpoints of $T_C + t_1/2$ and $T_C - t_1/2$. The ^1H scrambling pulses with x and y phases before gradient 4 are applied with an amplitude of 20 kHz and lengths of 1 and 0.2 ms. The gradient pulses with a half-sine shape are applied along the z-axis. The amplitudes and lengths are as follows: $Gr_1 = (3.6$ G/cm, 2 ms), $Gr_2 = (3$ G/cm, 0.5 ms), $Gr_3 = (18$ G/cm, 2 ms), $Gr_4 = (3$ G/cm, 2 ms), $Gr_5 = (21$ G/cm, 0.5 ms), $Gr_6 = (6$ G/cm , 2 ms), $Gr_7 = (6$ G/cm, 0.5 ms). The phase cycling is as follows: $\phi_1 = (x, -x)$, $\phi_2 = (4(x), 4(-x))$, $\phi_3 = (2(y), 2(-y))$, $\phi_4 = (8(x), 8(-x))$, $\phi_a = (x, -x, -x, x)$. Quadrature detection of the t_1 dimension is performed by changing ϕ_1 in the TPPI-States manner. The number of repetitions for T_{rel} is changed, i.e., 1, 2, 3, and 5. (b, bottom) Pulse sequence for measuring $^{13}C_\alpha-^1H_\alpha$ zero/double quantum relaxation rates. The amplitude of ^1H spin-locking by a continuous wave during the T_{rel} period was 5.2 kHz. T_{rel} was changed, i.e., 10, 20, 30, and 50 ms. Three different carrier positions for the $^{13}C_\alpha$ channel were used, as described in the text. All other parameters were the same as in (a), except for $\phi_3 = (2(x), 2(-x))$.

However, the relaxation rates of the tilted components are the averages of those of four orthogonal components:

$$R(H_{Z'}C_{Z''}) = (\cos^2\theta_H)(\cos^2\theta_C) R(H_{XY}C_{XY}) + (\sin^2\theta_H)(\cos^2\theta_C) R(H_Z C_{XY}) + (\cos^2\theta_H)(\sin^2\theta_C) R(H_{XY}C_Z) + (\sin^2\theta_H)(\sin^2\theta_C) R(H_Z C_Z)$$

where $R(X)$ is the relaxation rate of the X component. Since $R(H_{XY}C_{XY})$ is expected to be smaller than $R(H_Z C_{XY})$ and

(26) Kushlan, D. M.; LeMaster, D. M. *J. Biomol. NMR* **1993**, *3*, 701−708.
(27) Curley Jr., R. W.; Panigot, M. J.; Hansen, A. P.; Fesik, S. W. *J. Biomol. NMR* **1994**, *4*, 335−340.

Table 1. Relaxation Rates (s^{-1}) of the $^{13}C_\alpha$ Single Quantum ($^{13}C_Y$) and $^{13}C_\alpha-^{1}H_\alpha$ Zero/Double Quantum ($^{13}C_Y{}^{1}H_Y$) Coherences of Selected Peaks of the C-Terminal Domain of the α Subunit of *E. coli* RNA Polymerase at 10 °C in $^{2}H_2O$[a]

	$^{1}H_\alpha$ and other ^{2}H		all ^{1}H	
residue	$^{13}C_Y$	$^{13}C_Y{}^{1}H_Y$	$^{13}C_Y$	$^{13}C_Y{}^{1}H_Y$
V264*	104.3 (8.0)	14.0 (2.0)	94.4 (15.7)	29.9 (2.6)
A267*	87.9 (8.5)	18.1 (2.5)	81.3 (11.0)	39.0 (4.6)
T285	76.7 (7.3)	38.6 (2.9)	82.3 (8.5)	46.7 (5.3)
E286	77.9 (10.1)	22.7 (2.0)	51.5 (10.2)	36.2 (8.1)
V287*	91.6 (7.7)	13.9 (1.9)	95.8 (13.8)	36.2 (3.0)
E288	73.3 (6.0)	28.0 (3.3)	74.4 (8.7)	36.9 (3.6)
L295*	67.9 (7.9)	20.4 (1.1)	83.3 (14.4)	46.2 (3.6)
K297*	81.8 (9.4)	14.6 (1.3)	111.8 (12.0)	46.5 (4.9)
K298*	60.5 (8.4)	19.6 (1.6)	71.9 (7.7)	41.5 (3.9)
D305	57.4 (7.0)	26.8 (2.5)	62.4 (8.2)	34.5 (2.9)
V306*	67.7 (4.8)	15.3 (1.6)	75.1 (6.2)	34.2 (2.8)
A324*	58.7 (6.8)	15.5 (1.7)	56.4 (4.3)	23.6 (1.8)
average	75.5	20.6	78.4	37.6
average*	77.5	16.4	83.7	37.1

[a] The left two columns are for the selectively-$^{1}H_\alpha$- and uniformly-^{13}C-, -^{15}N-, and -^{2}H-labeled sample. The right two columns are for the uniformly-^{13}C- and -^{15}N-labeled sample. The values in parentheses are the errors of the relaxation rates. The average values are simple averages of all the 12 residues. The average* values are averages of the eight residues indicated by an asterisk, of which selective $^{1}H_\alpha$ labeling was achieved.

$R(H_{XY}C_Z)$, sufficiently small θ_H and θ_C are recommended for accurate measurement of $R(H_{XY}C_{XY})$. This is why we performed three experiments with different ^{13}C offsets. Because the purpose of these experiments was to show a large difference between the relaxation rates of single and double/zero quantum coherences, we made the rough assumption that $R(C_Z) = 0$, $R(H_{XY}C_Z) = R(H_ZC_{XY}) = R(C_{XY})$, and $R(H_ZC_Z) = 0$, instead of measuring individual rates. The relaxation rates of pure single and double/zero quantum coherences were calculated as

$$R(C_{XY}) = R(C_{Z''})/\cos^2\theta_C$$

$$R(H_{XY}C_{XY}) = [R(H_{Z'}C_{Z''}) - R(C_{XY})(\sin^2\theta_H \cos^2\theta_C + \cos^2\theta_H \sin^2\theta_C)]/(\cos^2\theta_H \cos^2\theta_C)$$

The relaxation rates of $^{13}C_\alpha$ nuclei in the rigid part of the molecule and of which the signals are separated well in the spectra are listed in Table 1. As an example, the first 2D spectrum on zero/double quantum relaxation measurement for the deuterated sample is shown in Figure 2. The single quantum relaxation experiment gave weaker peaks than this because of the losses in the additional conversion time for $^{13}C \leftrightarrow {}^{13}C-{}^{1}H$ states. The protonated sample gave even worse spectra because of more relaxation caused by the $^{1}H-{}^{1}H$ dipolar interaction and magnetization transfer through the $^{1}H-{}^{1}H$ scalar coupling when the Hartmann−Hahn matching condition is accidentally satisfied. This is why so few relaxation rates were obtained. The average transverse relaxation rate ($1/T_2$) of in-phase ^{13}C magnetization was 75.5 s^{-1}. Since the $^{1}H-{}^{13}C$ dipole−dipole interaction contributes predominantly to this value, it should not and actually did not depend on the type of labeling. This number corresponds to a rotational correlation time of 17 ns, as judged from the numerical simulation given in Figure 3, with the assumption of complete rigidity of the molecule. The correlation time calculated from the ^{15}N relaxation times measured at 30 °C in a $^{1}H_2O$ solution was 8.4 ns. The correlation time is simply proportional to the viscosity of the solvent in this case. The viscosity of $^{2}H_2O$ at 10 °C is 1.7 cP and that of $^{1}H_2O$ at 30 °C is 0.8 cP. This sample with the correlation time of 17 ns is appropriate for testing the effectiveness of the following experiments for proteins larger than 30 kDa. The correlation time of a 37 kDa Trp repressor/operator DNA complex was 13.4 ns at 37 °C. If it is dissolved in a $^{2}H_2O$ solution, the correlation time can be calculated to be 16 ns by multiplying by the ratio of the viscosities. Our test sample at 10 °C is similarly challenging as a 37 kDa molecule at 37 °C.

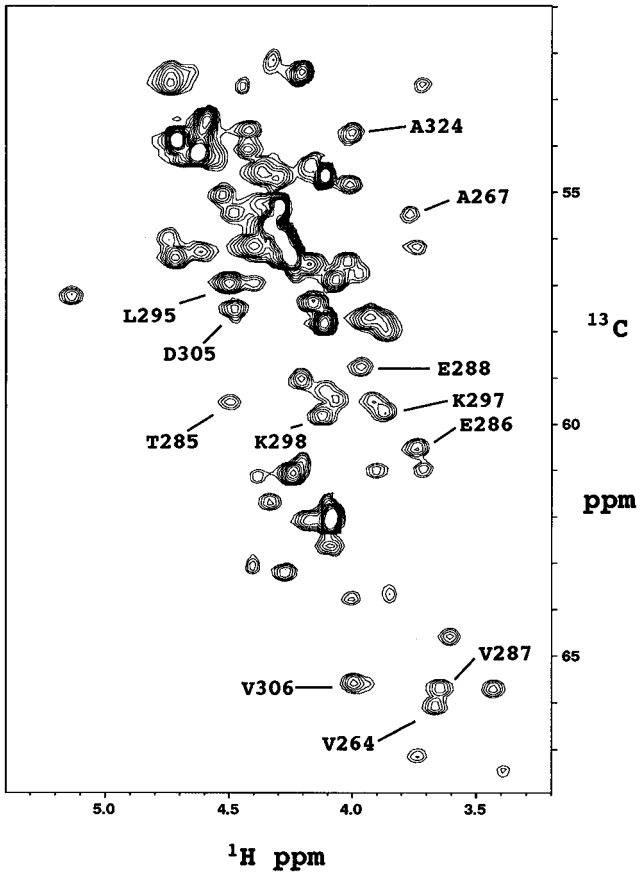

Figure 2. First 2D $^{1}H_\alpha-{}^{13}C_\alpha$ correlation spectrum for the $^{13}C_\alpha-{}^{1}H_\alpha$ zero/double quantum relaxation rate measurement. The sample was the $^{1}H_\alpha$-selectively-labeled [^{2}H]-, [^{13}C]-, and [^{15}N]protein. The relaxation rates were determined from the peaks labeled with their residue names.

The relaxation rates of the double/zero quantum coherences for the ^{13}C, ^{15}N labeled protein, which has all ^{1}H nuclei, were substantially slower than those of ^{13}C transverse magnetization, as shown in Table 1. The contribution by the $^{13}C-{}^{1}H$ dipole−dipole interaction is very small, i.e., only 1%, in this case. A large contribution is made by the $^{1}H-{}^{1}H$ dipole−dipole interaction with surrounding ^{1}H nuclei. The simulated value for a 17 ns correlation time was 52 s^{-1}, as shown in Figure 3. The relaxation rates obtained experimentally are considerably smaller than the simulated ones. The difference could be explained by the dynamics of interproton vectors, which is not considered in the simulation.

For the $^{1}H_\alpha$-selectively-labeled ^{2}H sample, the relaxation rates again became slower. Because of the statistical distribution of ^{1}H and ^{2}H in the side chains, which could be generated through the metabolism of amino acids, the relaxation curve may not be single exponential. The relaxation rates obtained here were statistical averages. Especially for the amino acids labeled properly, i.e., Lys, Leu, and Val, the relaxation rates became half those of the fully protonated sample. Even for Glu and Asp, considerable improvement was observed. This is probably due to dilution of surrounding ^{1}H spins, though it is not easy to

obtain a good estimate of the contribution by the residual ^{1}H spins. The simulated value for the fully deuterated molecule except for the $^1H_\alpha$ spin was 9.4 s^{-1}, as shown in Figure 3. In this simulation, a large contribution is made by the dipole−dipole interaction between the ^{1}H spin in a zero/double quantum state and ^{13}C spins other than the counterpart of the ^{1}H spin. The ^{13}CO and $^{13}C_\beta$ nuclei are relatively close to the ^{1}H spin. However, half of the relaxation remains unexplained. This is probably due to residual ^{1}H spins, and $^1H_\alpha$ spins in other residues. Perfect selective $^1H_\alpha$ labeling for all of the amino acids may give relaxation times as long as the simulated values. Even with incomplete labeling, long enough relaxation times of the $^1H_\alpha-^{13}C_\alpha$ double/zero quantum coherences were obtained for application to correlation experiments for backbone nuclei which need mixing times of 50 ms.

Backbone Resonance Assignment. The 3D HACAN experiment connects the $^{13}C_\alpha-^1H_\alpha$ zero/double quantum coherences to amide ^{15}N spins. The pulse sequence is shown in Figure 4a. Two cross peaks arise from a $^{13}C_\alpha-^1H_\alpha$ pair, which correspond to intraresidue ^{15}N and ^{15}N in the succeeding residue. The coherence transfer pathway is described as

$$H_Y^{(i)} \rightarrow H_Y^{(i)}C_Y^{(i)}(t_1) \rightarrow H_Z^{(i)}C_Z^{(i)}N_Y^{(i)}(t_2) \rightarrow H_Y^{(i)}C_Y^{(i)} \rightarrow H_X^{(i)}(t_3)$$

$$H_Y^{(i)} \rightarrow H_Y^{(i)}C_Y^{(i)}(t_1) \rightarrow H_Z^{(i)}C_Z^{(i)}N_Y^{(i+1)}(t_2) \rightarrow H_Y^{(i)}C_Y^{(i)} \rightarrow H_X^{(i)}(t_3)$$

where H denotes the $^1H_\alpha$ spin, C denotes the $^{13}C_\alpha$ spin, and N denotes the ^{15}N spin. The superscripts, (i) and (i+1), represent residue numbers. Since during the mixing time for $^{13}C_\alpha{}^{(i)}-^{15}N^{(i)}$ scalar coupling the $^{13}C_\alpha$ magnetization is dephased to the antiphase term with respect to $^{13}C_\beta$ and is refocused during each of the two mixing periods, the $^{13}C_\alpha-^{13}C_\beta$ coupling should also be taken into account for optimization of the length of the $^{15}N-^{13}C_\alpha$ mixing times. ^{1}H spin-locking is applied during these periods to suppress $^1H-^1H$ scalar coupling evolution for the amino acid residues which are protonated at H_β. During t_2, the ^{15}N chemical shift evolution period, a $H_ZC_ZN_Y$ state is generated. For a fully protonated sample, this term relaxes relatively fast through $^1H-^1H$ cross relaxation to the surrounding ^{1}H spins. However, for a deuterated sample, the H_Z component can survive long. Another choice for the state during the t_2 period is the C_ZN_Y term, by refocusing the $^{13}C_\alpha$ antiphase term with respect to $^1H_\alpha$ at the end of the $^{13}C_\alpha-^{15}$N mixing period. This term is not affected by the problem caused by ^{1}H cross relaxation even for the protonated sample. But the former type of pulse sequence is preferable. Since the single quantum coherence of $^{13}C_\alpha$ decays very quickly, even the period of 3.4 ms for refocusing of the antiphase term reduces the signal intensity. Deuterium decoupling is applied during the ^{15}N chemical evolution time using a continuous wave flanked by $\pi/2$ pulses to maintain the magnetization of the ^{2}H spin of the solvent. This treatment gives smoother recovery of the ^{2}H signal for the static field lock system. The lock is trapped during the deuterium decoupling and restarted after gradient 6. At the midpoint of the t_2 period, a pair of $^{13}C_\alpha$ $\pi/2$ pulses are applied which invert $^{13}C_\alpha$ and ^{13}CO simultaneously for decoupling the $^{15}N-^{13}C_\alpha$ and $^{15}N-^{13}$CO couplings. The last ^{1}H pulse is applied for better suppression of the solvent signal.[28]

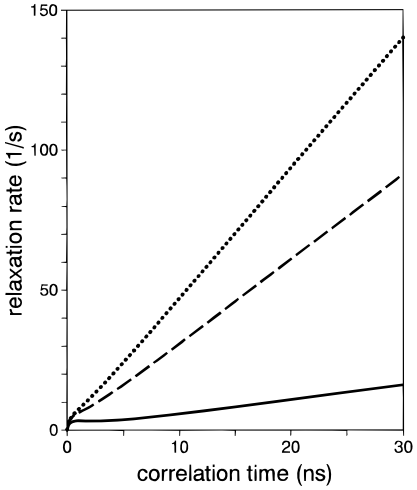

Figure 3. Simulation of the relaxation rates of the $^{13}C_\alpha$ single quantum and $^{13}C_\alpha-^1H_\alpha$ zero/double quantum states. Complete rigidity of the molecule and isotropic overall tumbling are assumed. The correlation time represents the life time of the second-order spherical harmonic distribution of the molecular orientation, as usual. The solid line is the average relaxation rate of the $^{13}C_\alpha-^1H_\alpha$ zero and double quantum coherences in the selectively-$^1H_\alpha$- and uniformly-^{13}C-, -^{15}N-, and -^{2}H-labeled sample. The broken line is the average relaxation rate of the $^{13}C_\alpha-^1H_\alpha$ zero and double quantum coherences in the uniformly-^{13}C- and -^{15}N-labeled sample. The dotted line is the relaxation rate of the $^{13}C_\alpha$ single quantum coherence. The dipole−dipole interactions between $^1H_\alpha-^{13}C_\alpha$, $^1H_\alpha$-surrounding H (^{1}H or ^{2}H) nuclei, $^1H_\alpha$-surrounding ^{13}C nuclei, $^{13}C_\alpha$-surrounding H (^{1}H or ^{2}H) nuclei, and $^{13}C_\alpha$-neighboring ^{13}C nuclei are included. The chemical shift anisotropy of $^{13}C_\alpha$ is also included. A distance between $^1H_\alpha$ and $^{13}C_\alpha$ of 0.109 nm, a distance between $^{13}C_\alpha$ and neighboring ^{13}C nuclei of 0.153 nm, an effective distance of the surrounding H (^{1}H or ^{2}H) nuclei from $^1H_\alpha$ of 0.197 nm, an effective distance of the surrounding H nuclei from $^{13}C_\alpha$ of 0.181 nm, an effective distance of surrounding ^{13}C from $^1H_\alpha$ of 0.179 nm, and ^{13}C chemical shift anisotropy with a difference of 34 ppm between parallel and perpendicular components are used. The effective distance is $(\Sigma_i r_i^{-6})^6$, where r_i are interspin distances. The resonance frequency of ^{1}H is set at 600 M Hz. The cross-correlations between different mechanisms are ignored.

The 3D HACACO experiment connects the $^{13}C_\alpha-^1H_\alpha$ zero/double quantum coherence to the intraresidue ^{13}CO spin as

$$H_Y \rightarrow H_YC_Y(t_1) \rightarrow H_ZC_ZC'_Y(t_2) \rightarrow H_YC_Y \rightarrow H_X(t_3)$$

where C' represents the ^{13}CO spin and other spins are the same as in the case of HACAN. All spins are in the same residue. The pulse sequence is shown in Figure 4b. Most of the features are the same as in the case of HACAN, except that ^{15}N is replaced by ^{13}CO. Note that selective pulses are used for the coherence transfer between $^{13}C_\alpha$ and ^{13}CO. Also note that the refocusing pulses of $^{13}C_\alpha$ during 2 T_C must cover the chemical shift range of $^{13}C_\beta$ spins. The length of the $^{13}C_\alpha-^{13}$CO mixing time is adjusted to $1/J_{CC}$ for refocusing of the antiphase term with respect to $^{13}C_\beta$, where J_{CC} is the coupling constant between $^{13}C_\alpha$ and $^{13}C_\beta$. As $^{13}C_\alpha-^{13}$CO scalar coupling is larger than J_{CC}, the selective ^{13}CO π pulse is positioned so as to maximize the antiphase term with respect to ^{13}CO. The π pulses at the beginning of the first $2T_C$ period and at the end of the second $2T_C$ period are applied to compensate for the phase shift of the $^{13}C_\alpha$ signals caused by the other ^{13}CO π pulses. Because of the same effect during the ^{13}CO chemical shift evolution caused

(28) Kay, L. E. *J. Am. Chem. Soc.* **1993**, *115*, 2055.
(29) Fujiwara, T.; Nagayama, K. *J. Magn. Reson.* **1988**, *77*, 53−63.
(30) Fujiwara, T.; Nagayama, K. *J. Magn. Reson.* **1993**, *A104*, 103−105.
(31) Geen, H.; Freeman, R. *J. Magn. Reson.* **1991**, *93*, 93−141.

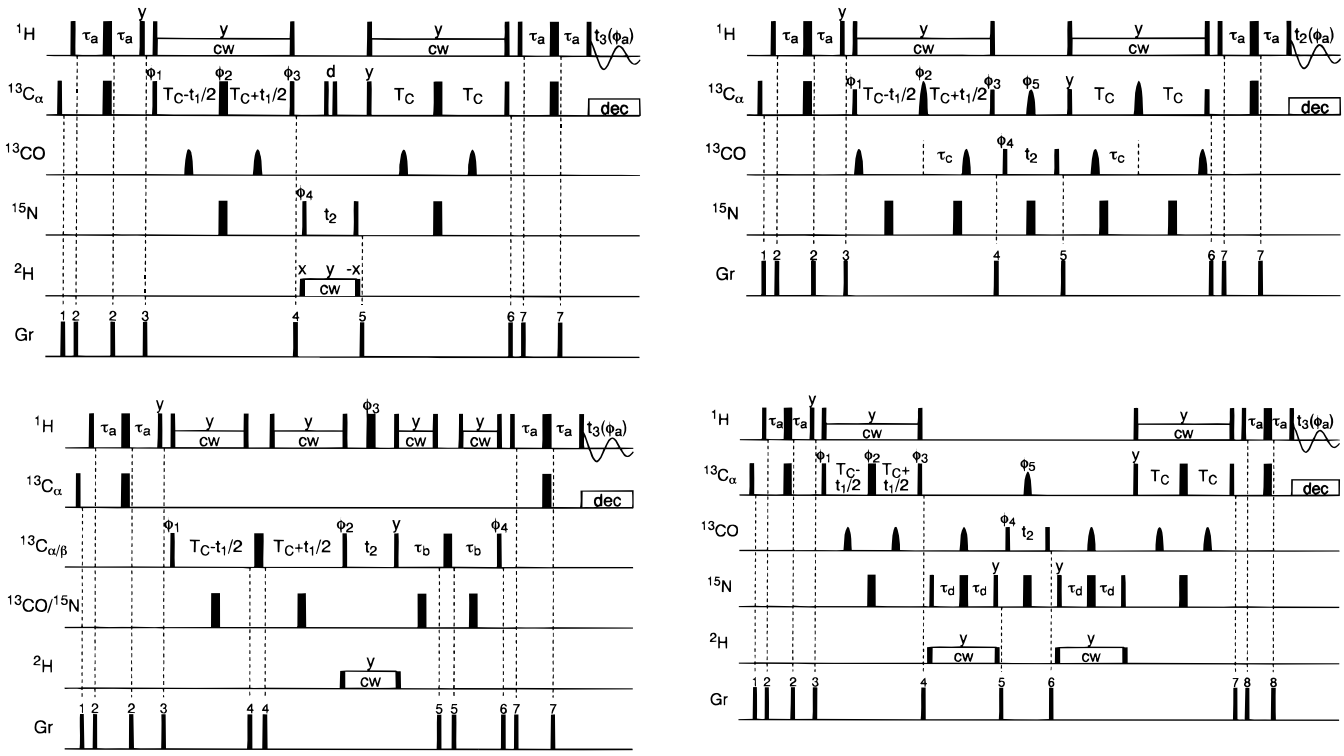

Figure 4. (a, top left) Pulse sequence for the HACAN experiment. The carriers of the four channels for ^{1}H, ^{13}C, ^{15}N, and ^{2}H were positioned at 4.48, 57.5, 118.3, and 8 ppm, respectively. Thin and thick bars represent the $\pi/2$ and π pulses. All pulses without phase are applied in the *x*-direction. The $\pi/2$ pulse width of ^{1}H pulses is 6.6 μs, and the amplitude of ^{1}H spin-locking by a continuous wave is 6.8 kHz. The $\pi/2$ pulse width of $^{13}C_\alpha$ pulses is 15.3 μs, and the amplitude of decoupling by the WALTZ16 sequence is 2.1 kHz. The ^{13}CO selective π pulses are generated from the same ^{13}C channel by phase modulation centered at 176.5 ppm. They are applied at the midpoints of the $T_C - t_1/2$, $T_C + t_1/2$, and T_C periods. A Gaussian shape with a maximum amplitude of 5.2 kHz is used. The $\pi/2$ pulse width of ^{15}N pulses is 43 μs. The ^{2}H pulses and decoupling by a continuous wave are applied with an amplitude of 1.25 kHz. The delays are as follow: $\tau_a = 1.7$ ms, $T_C = 13$ ms, $d = 47.2$ μs ($=1/(f_{C\alpha} - f_{CO}) - (4/\pi)\tau_{C90}$, where $f_{C\alpha}$ and f_{CO} are the offsets of $^{13}C_\alpha$ and ^{13}CO, and τ_{C90} is the ^{13}C $\pi/2$ pulse width). The phases of pulses are cycled as $\phi_1 = (2(x), 2(-x))$, $\phi_2 = (x, -x)$, $\phi_3 = (4(y), 4(-y))$, $\phi_4 = (x, -x)$, $\phi_a = (x, -x, -x, x, -x, x, x, -x)$. The quadrature detection of t_1 is achieved by TPPI-States with ϕ_1, and that of t_2 with ϕ_4. The gradients with a half-sine shape are $Gr_1 = (y, 2.5$ G/cm, 1 ms), $Gr_2 = (y, 10$ G/cm, 1 ms), $Gr_3 = (z, 30$ G/cm, 1 ms), $Gr_4 = (x, 25$ G/cm, 1 ms), $Gr_5 = (x, -10$ G/cm, 1 ms), $Gr_6 = (z, -10$ G/cm, 1 ms), $Gr_7 = (z, 17.5$ G/cm, 1 ms). (b, top right) Pulse sequence for the HACACO experiment. The ^{1}H carrier is positioned at 4.28 ppm. The ^{13}C carrier is first positioned at 57.5 ppm, then moved to 176.5 ppm before gradient 4, and finally moved back to 57.5 ppm before gradient 5. The ^{15}N carrier is positioned at 118.3 ppm. The ^{1}H pulse and spin-locking are the same as in the case of HACAN. The $^{13}C_\alpha$ selective $\pi/2$ pulses, represented by short thin bars, are applied with an amplitude of 3.9 kHz. The taller shaped π pulses on $^{13}C_\alpha$ during the $2T_C$ periods are REBURP pulses[31] with a maximum amplitude of 15.4 kHz. The shorter shaped π pulse on $^{13}C_\alpha$ at the midpoint of the t_2 period is a Gaussian-shaped pulse with a maximum amplitude of 5.2 kHz and phase modulation centered on $^{13}C_\alpha$. The short ^{13}CO selective π pulses are Gaussian-shaped pulses with a maximum amplitude of 5.2 kHz and phase modulation centered on ^{13}CO. The ^{13}CO short $\pi/2$ pulses are rectangular pulses with an amplitude of 3.9 kHz. The ^{15}N π pulses with the same amplitude as in the case of HACAN are applied at the midpoints of the $T_C - t_1/2$, $T_C + t_1/2$, and T_C periods. The delays τ_a and T_C are the same as in the case of HACAN. τ_c is 9.7 ms. The gradients and the quadrature detection are the same as in the case of HACAN. The phases of pulses are cycled as $\phi_5 = (2(x), 2(-x))$ in addition to those for HACAN. (c, bottom left) Pulse sequence for HACACB. The conditions for ^{1}H are the same as in the case of HACAN. The ^{13}C carrier is first positioned at 57.5 ppm, then moved to 42.5 ppm before gradient 3, and finally moved back to 57.5 ppm before gradient 6. The ^{2}H carrier is positioned at 3 ppm. The other conditions for ^{13}C, ^{15}N, and ^{2}H are the same as for HACAN. $T_C = 21.5$ ms, $\tau_a = 1.5$ ms, and $\tau_b = 7.2$ ms. The ^{13}CO selective π pulses and ^{15}N π pulses are applied at the midpoints of $T_C - t_1/2$, $T_C + t_1/2$, and τ_b. The ^{13}CO selective π pulse is the same as in the case of HACAN. The conditions for ^{2}H are the same as for HACAN. The phase cycling is $\phi_1 = (x, -x)$, $\phi_2 = (4(y), 4(-y))$, $\phi_3 = (x, -x)$, $\phi_4 = (2(x), 2(-x))$, $\phi_a = (x, -x, -x, x)$. The quadrature detection of t_1 is made by TPPI-States with ϕ_1. The quadrature detection of t_2 is made by TPPI-States with $\pi/2$ increments of ϕ_1 and ϕ_2 simultaneously. The gradients are $Gr_1 = (y, 2.5$ G/cm, 1 ms), $Gr_2 = (y, 10$ G/cm, 0.5 ms), $Gr_3 = (z, 30$ G/cm, 1 ms), $Gr_4 = (x, 10$ g/cm, 0.5 ms), $Gr_5 = (x, 30$ G/cm, 0.5 ms), $Gr_6 = (z, 10$ G/cm, 1 ms), $Gr_7 = (z, 17.5$ G/cm, 0.5). (d, bottom right) Pulse sequence for HACA(N)CO. The ^{1}H pulses and spin-lockings are the same as in the case of HACAN. The ^{13}C carrier is first positioned at 57.5 ppm, then moved to 176.5 ppm before gradient 4, and finally moved back to 57.5 ppm after the $\pi/2$ pulse at the end of τ_d. The τ_d delay is 12 ms. All rectangular pulses and shaped pulses are the same as for HACACO. The conditions for ^{15}N and ^{2}H are the same as for HACAN. The phase cycling of pulses and quadrature detection are the same as for HACACO. The gradients are $Gr_1 = (y, 2.5$ G/cm, 1 ms), $Gr_2 = (y, 10$ G/cm, 1 ms), $Gr_3 = (z, 30$ G/cm, 1 ms), $Gr_4 = (z, -15$ G/cm, 1 ms), $Gr_5 = (x, 25$ G/cm, 1 ms), $Gr_6 = (x, 10$ G/cm, 1 ms), $Gr_7 = (z, 10$ G/cm, 1 ms), $Gr_8 = (z, 12.5$ G/cm, 1 ms).

by the $^{13}C_\alpha$ selective π pulse, the phase shift should be compensated for in the data processing. Deuterium decoupling is not required in this experiment.

The 3D HACACB experiment connects the $^{13}C_\alpha - ^1H_\alpha$ zero/double quantum coherence to the intraresidue $^{13}C_\beta$ spin as

$$H_Y \rightarrow H_Y C_Y(t_1) \rightarrow H_Z C_Z B_Y(t_2) \rightarrow H_Y C_Y \rightarrow H_X(t_3)$$

where *B* represents the $^{13}C_\beta$ spin and other spins are the same as in the case of HACAN. All spins are in the same residue. The pulse sequence is shown in Figure 4c. Most of the features are the same as in the case of the HACAN and HACACO experiments. For optimal sensitivity of the $^{13}C_\beta$ peak, the length of the $^{13}C_\alpha - ^{13}C_\beta$ mixing period should be $(2n + 1)/(2J_{CC})$. The first mixing period is $3/(2J_{CC})$ for obtaining a longer $^{13}C_\alpha$ chemical shift evolution time. During the $^{13}C_\beta$ chemical shift evolution time, deuterium decoupling is applied to the aliphatic

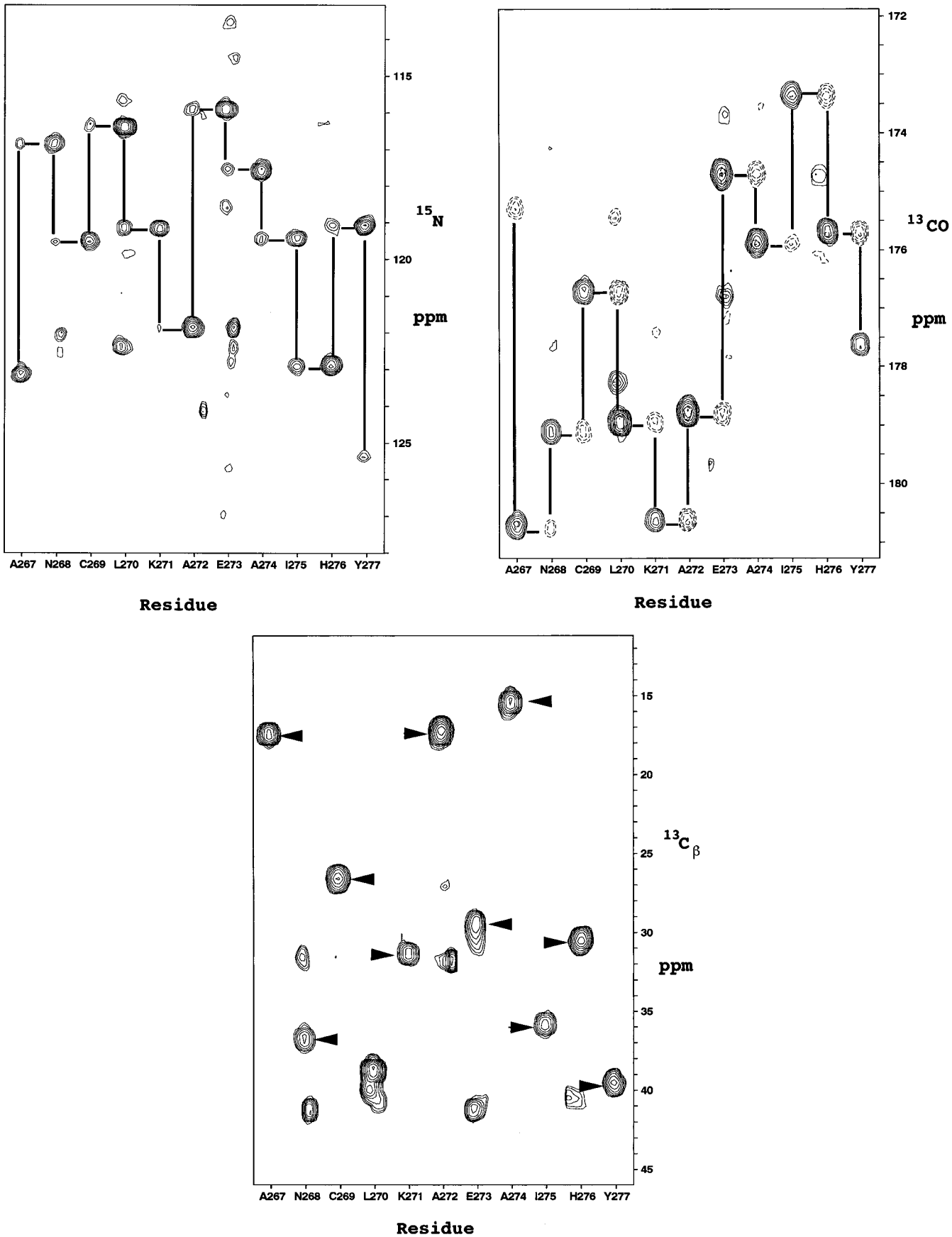

Figure 5. Strip plots for the residues from A267 to Y277. The contour levels exponentially increase by a factor of 1.41. (a, top left) A strip plot of the 3D HACAN spectrum. (b, top right) An overlaid strip plot of the 3D HACACO spectrum, solid contour lines, and the 3D HACA(N)CO spectrum, broken ones. (c, bottom) A strip plot of the 3D HACACB spectrum. Arrows indicate the corresponding $^{13}C_\beta$ peaks.

^{2}H spins using the same scheme as described above. A ^{1}H π pulse is also applied at the midpoint of t_2 to decouple ^{1}H attached to $^{13}C_\beta$, because some of the amino acids have ^{1}H in their side chains.

The 3D HACA(N)CO experiment connects the $^{13}C_\alpha-^{1}H_\alpha$ zero/double quantum coherence through the intraresidue ^{15}N spin to the previous ^{13}CO spin, and through the ^{15}N of the succeeding residue to the ^{13}CO spin in the same residue as $^{13}C_\alpha$. The coherence transfer pathway is

$$H_Y^{(i)} \rightarrow H_Y^{(i)}C_Y^{(i)}(t_1) \rightarrow H_Z^{(i)}C_Z^{(i)}N_Y^{(i)} \rightarrow H_Z^{(i)}C_Z^{(i)}N_Z^{(i)}C'_Y{}^{(i-1)}(t_2) \rightarrow H_Z^{(i)}C_Z^{(i)}N_Y^{(i)} \rightarrow H_Y^{(i)}C_Y^{(i)} \rightarrow H_X^{(i)}(t_3)$$

$$H_Y^{(i)} \rightarrow H_Y^{(i)}C_Y^{(i)}(t_1) \rightarrow H_Z^{(i)}C_Z^{(i)}N_Y^{(i+1)} \rightarrow H_Z^{(i)}C_Z^{(i)}N_Z^{(i+1)}C'_Y{}^{(i)}(t_2) \rightarrow H_Z^{(i)}C_Z^{(i)}N_Y^{(i+1)} \rightarrow H_Y^{(i)}C_Y^{(i)} \rightarrow H_X^{(i)}(t_3)$$

The total length of the pulse sequence is more than 100 ms, because coherence is transferred in a relayed manner through relatively small $^{13}C_\alpha-^{15}N$ and $^{15}N-^{13}CO$ coupling constants. Nevertheless, most of the correlation peaks to the preceding residues, which are given by the upper transfer pathway, appeared with good sensitivity. As the ^{15}N nuclei are attached by ^{2}H, the relaxation time of the ^{15}N transverse magnetization is considerably long. As calculated from the ^{15}N chemical shift anisotropy and the $^{15}N-^{2}H$ dipolar interaction, the relaxation time is expected to be more than 200 ms for this molecule. For this reason, the efficiency of the correlation from ^{15}N to ^{13}CO, which is governed by the ^{15}N relaxation rate, is high, compared with that in the case of the HA(CACO)N experiment. Deuterium decoupling is applied while the ^{15}N transverse component is being generated.

The spectra obtained in the above four experiments showed signals of good quality. The sequential connectivities to the ^{15}N and ^{13}CO spins were weaker, but most of them appeared clearly. However, they also had several common shortcomings. Pro and Gly residues gave no signals. Pro residues were fully deuterated, including H_α. The magnetization of Gly residues decayed because of the fast relaxation caused by the extra ^{1}H spin. Ser266 and Ser299 gave almost no signals. The assignments made at 30 °C suggest that for these Ser residues, the $^{13}C_\alpha$ and $^{13}C_\beta$ spins have similar chemical shifts. During the constant time period, the $^{13}C_\alpha$ magnetization was lost through a strong coupling effect. Peaks of the $^{1}H_\alpha-^{13}C_\alpha$ spins in the residues preceding Pro were always weaker. The reason was not identified, but higher rigidity of this part of the molecule or a special scalar coupling network of the spins could cause the decrease of the peak intensity. Ile278 gave weaker peaks because its $^{1}H_\alpha$ offset (3.39 ppm) was far from the ^{1}H spin-locking frequency. As mentioned by Grzesiek and Bax,[18] a relatively strong spin locking field was required to suppress the $^{1}H_\alpha-^{13}C_\alpha$ coupling for the full range of $^{1}H_\alpha$ chemical shifts. The $^{1}H_\alpha$ chemical shift range of this protein is relatively small because it is mainly composed of α-helices. For proteins having *β*-sheets, a stronger ^{1}H spin-locking field is recommended. Interestingly, most residues that were not properly labeled, which were probably fully protonated, also gave good signals. This could be explained by the fact that most of the protonated residues are located on the surface of the molecule and exhibit less relaxation due to their dynamics, because these residues are hydrophilic.

A strip plot of the HACAN spectrum is shown in Figure 5a. In the column for each $^{13}C_\alpha-^{1}H_\alpha$ pair, a stronger intraresidue ^{15}N peak and a weaker one connecting to the ^{15}N spin in the succeeding residue appeared. The sequential peak exhibits a quarter or a third of the intensity of the intraresidue peak. These peaks can be traced along the primary sequence, as shown in the figure. An overlap display of strip plots of the HACACO and HACA(N)CO spectra is shown in Figure 5b. In each column, HACACO gives an intraresidue ^{13}CO peak, as shown by solid contours, and HACA(N)CO gives the ^{13}CO peak of the preceding residue shown by broken contours. HACA(N)-CO gave much weaker intraresidue ^{13}CO peaks as well, but they are covered by HACACO peaks in the plot. The intraresidue and sequential ^{13}CO peaks can be traced along the primary sequence as shown in Figure 5b. A strip plot of the HACACB spectrum is shown in Figure 5c. This experiment gave similarly good sensitivity to that of the HACACO experiment.

The intensities of intraresidue peaks in the HACAN, HACACO, and HACACB spectra were very high. For the backbone sequential assignment, either sequential peaks on HACAN or peaks on HACA(N)CO were also required. Most of them were observed, though they were weaker than intraresidue peaks. Except for the amino acid-specific incompleteness mentioned above, only two of the sequential connectivities of Thr301 and Glu302 in the HACAN spectrum were missing, and none of the sequential peaks were missing in the HCA(N)CO spectrum. The ^{13}CO sequential connectivities obtained on HACA(N)CO were more intense than the ^{15}N sequential connectivities on HACAN.

Conclusion

Using a selectively-$^{1}H_\alpha$-and uniformly-^{13}C-, ^{15}N-, and ^{2}H-labeled protein, and the newly developed triple resonance experiments, the sequential connectivities of $^{13}C_\alpha-^{1}H_\alpha$ spin pairs were obtained in duplicate through ^{15}N and through ^{13}CO spins. Actual assignments were successfully made for the C-terminal domain of the α subunit of *E. coli* RNA polymerase under the condition that the molecule tumbles slowly. Through improvement of the labeling method, further sensitivity improvement would be expected. For larger proteins in a high pH solution or at high temperature, where the amide protons exchange too fast, the present method is the only realistic means of backbone resonance assignment. The success of these experiments implies the following future directions. Starting from $^{13}C_\alpha-^{1}H_\alpha$ assignments, side chain ^{13}C assignments can be made with the ^{13}C TOCSY scheme using the same sample. This would give higher sensitivity than that of the CC(CO)NH experiment, which is used for a nonselectively-^{2}H-labeled sample. Selective ^{1}H labeling of other side chain nuclei would be useful for the assignment of the ^{1}H nuclei and for obtaining structural information from the ^{1}H spins for larger proteins.

JA962945F